

# The Nature of Singularity in Bianchi I Cosmological String Gravity Model with Second Order Curvature Corrections

S.Alexeyev, A.Toporensky, V.Ustiansky

*Sternberg Astronomical Institute, Moscow State University, Universitetsky Prospekt, 13,  
Moscow 119899, Russia*

We investigate Bianchi I cosmological model in the theory of a dilaton field coupled to gravity through a Gauss-Bonnet term. Two type of cosmological singularity are distinguished. The former is analogous to the Einstein gravity singularity, the latter (which does not appear in classical General Relativity) occurs when the main determinant of the system of field equations vanishes. An analogy between the latter cosmological singularity and the singularity inside a black hole with a dilatonic hair is discussed. Initial conditions, leading to these two types of cosmological singularity are found via numerical integration of the equation of motion.

General Relativity (GR) as leading theory of gravitational interaction at the classical level demonstrates a lot of interesting properties, for example, the existence of space time singularities [1]. The main “negative” feature of GR is that it is not renormalisable, so, it can not be quantized by the usual quantum field theory methods. The possible way to construct the quantum theory of gravity is to use string/M theory as the most promising candidate for the “theory of all physical interactions”. After compactification to four dimensional space time one obtains some effective gravitational theory which includes GR as the zeroth perturbation. This approach contains more wide set of solutions, and, hence, in addition to the singularity classes introduced by GR can include new types of singular behavior.

The simplest version of effective four dimensional string gravity action with the higher order curvature corrections up to the second order contains a coupling of the dilaton with gravity via the Gauss-Bonnet term as follows [2] (we use the units where  $m_{PL}/\sqrt{8\pi} = 1$ ):

$$S = \int d^4x \sqrt{-g} \left[ -\frac{1}{2}R + \frac{1}{2}\partial_\mu\phi\partial^\mu\phi + \frac{\lambda}{16}e^{-2\phi}S_{GB} \right], \quad (1)$$

where  $R$  is Ricci scalar,  $\phi$  is dilaton,  $\lambda$  is dilatonic string coupling constant which is positive. Second

order curvature correction  $\lambda e^{-2\phi}S_{GB}$  represents the product of the coupling functions  $e^{-2\phi}$  and Gauss-Bonnet combination  $S_{GB} = R_{ijkl}R^{ijkl} - 4R_{ij}R^{ij} + R^2$ . The solutions of this model have extensively been studied in the literature, both in a perturbative [3] and numerical [4,5] approaches.

One important aspect is that when the second order curvature correction is taken into account a wide class of solutions contains new types of singularities (earlier it was studied in  $d \geq 4$  space time case, see, for instance, [6] and references therein). For example, during the investigation of the black hole solution (asymptotically flat, spherically symmetric and static) a new type of black hole inner singularity was found. It occurs at the finite (non zero) radius inside black hole and has the topology  $S^2 \times R^1$  (an infinite tube in time direction). This is curvature singularity, though it is weak in Tipler’s terminology [7]. If one works in curvature gauge

$$ds^2 = \Delta dt^2 - \frac{\sigma^2}{\Delta} dr^2 - r^2(d\theta^2 + \sin^2\theta d\varphi^2),$$

where  $\Delta = \Delta(r)$  and  $\sigma = \sigma(r)$ , Einstein-Lagrange equations can be written in a matrix form

$$a_{i1}\Delta'' + a_{i2}\sigma' + a_{i3}\phi'' = b_i, \quad (2)$$

where  $i = 1, 2, 3$ ,  $a_{ij} = a_{ij}(\Delta, \Delta', \sigma, \phi, \phi')$  and  $b_i = b_i(\Delta, \Delta', \sigma, \phi, \phi')$ .

The describing singularity (we will call it as “determinant singularity”) occurs when the second part (in quadratic brackets) of the main system determinant

$$D_{main} = \Delta \left[ A\Delta^2 + B\Delta + C \right], \quad (3)$$

( $A$ ,  $B$  and  $C$  depend upon  $\Delta'$ ,  $\sigma$ ,  $\phi$ ,  $\phi'$ ) vanishes. The asymptotic behavior of the metric and dilaton functions near this singularity  $r_s$  is [5]

$$\begin{aligned} \Delta &= d_s + d_1(\sqrt{r-r_s})^2 + d_2(\sqrt{r-r_s})^3 + \dots, \\ \sigma &= \sigma_s + \sigma_1\sqrt{r-r_s} + \sigma_2(\sqrt{r-r_s})^2 + \dots, \\ \phi &= \phi_s + \phi_1(\sqrt{r-r_s})^2 + \phi_2(\sqrt{r-r_s})^3 + \dots, \end{aligned} \quad (4)$$

where  $d_i$ ,  $\sigma_i$ ,  $\phi_i$  are numerical factors and  $r - r_s \ll 1$ .

A numerical example is shown on Fig. 1(a,b) taken from [5]. The solution was obtained with the help of the numerical method based on the integration over an additional parameter along the solution trajectory described in Ref. [5]. Some new mathematical aspects of this strategy were additionally studied in Ref [8]. The solution consists of two branches which merge at determinant singularity  $r_s$  and solution could not be continued further in radial coordinate. It is necessary to point out that all the metric functions (independently of their maximal derivative order) work as  $\text{const}/\sqrt{r-r_s}$  in Riemannian tensor, therefore, cutvature square  $I = R_{ijkl}R^{ijkl}$  diverges.

The main goal of this paper is to indicate that this kind of singularity is also significant in cosmology. Previously, it was found in rather complicated models such as those elaborated to describe a dynamical compactification (we think that it is the first appearance of this kind of singularity in cosmology) [10], in multidimensional Lovelock gravity [11] and in Bianchi I [12,13] and Bianchi IX [13] with moduli fields. In our paper we show that the determinant singularity occurs in the Bianchi I cosmology (the line element is

$$ds^2 = dt^2 - a^2(t)dx_1^2 - b^2(t)dx_2^2 - c^2(t)dx_3^2, \quad (5)$$

$a(t)$ ,  $b(t)$ ,  $c(t)$  are the scale factors) in the theory with the simplest stringy motivated second order curvature correction (1).

Introducing three Hubble parameters  $p(t)$ ,  $q(t)$ ,  $r(t)$  according to following definition

$$p(t) = \frac{\dot{a}}{a}, \quad q(t) = \frac{\dot{b}}{b}, \quad r(t) = \frac{\dot{c}}{c},$$

where the dot denotes  $d/dt$ , the variation of action (1) with respect to the metric components and the dilaton field gives the following equations of motion:

$$pq + qr + rp + 24\dot{f}pqr - \dot{\phi}^2/2 = 0, \quad (6)$$

$$\begin{aligned} (1 + 8r\dot{f})(\dot{q} + q^2) + (1 + 8q\dot{f})(\dot{r} + r^2) \\ + (1 + 8\dot{f})qr + \dot{\phi}^2/2 = 0, \end{aligned} \quad (7)$$

$$\begin{aligned} (1 + 8r\dot{f})(\dot{p} + p^2) + (1 + 8p\dot{f})(\dot{r} + r^2) \\ + (1 + 8\dot{f})rp + \dot{\phi}^2/2 = 0, \end{aligned} \quad (8)$$

$$\begin{aligned} (1 + 8q\dot{f})(\dot{p} + p^2) + (1 + 8p\dot{f})(\dot{q} + q^2) \\ + (1 + 8\dot{f})pq + \dot{\phi}^2/2 = 0, \end{aligned} \quad (9)$$

$$\begin{aligned} \ddot{\phi} = -(p + q + r)\dot{\phi} + 8f'(\dot{p}qr + p\dot{q}r \\ + pqr\dot{r} + pqr(p + q + r)), \end{aligned} \quad (10)$$

where  $f(t) = \frac{\lambda}{16}e^{-2\phi}$ , and the prime denotes differentiation with respect to  $\phi$ . For mostly obvious presentation of the numerical results one have to introduce new variables  $h(t)$ ,  $\alpha(t)$ ,  $\beta(t)$

$$p = h + \alpha + \sqrt{3}\beta, \quad q = h + \alpha - \sqrt{3}\beta, \quad r = h - 2\alpha,$$

where  $h$  is a generalization of a Hubble parameter of the isotropic case and describes the expansion rate of the universe,  $\alpha$  and  $\beta$  are parameters of anisotropy.

It should be emphasized that the presence of the Gauss-Bonnet term can in principle allow the violation of the weak energy condition [4]. This means that it is possible for the spatially flat universe to make a transition from expansion to contraction (see, for example, [9]) what can also be easily seen directly from the constraint equation (6). Indeed, in Einstein gravity the geometrical part of constraint (6) is  $3h^2 - 3\alpha^2 - 3\beta^2$  which is nonpositive if  $h = 0$  and, hence, this case is inconsistent with the constraint equation. Even if the Gauss-Bonnet term is taken into account in the isotropic case the correction  $24\dot{f}pqr$  vanishes at  $h = 0$ , so the Einstein gravity result ( $h$  can not change it's sign in the spatially flat homogeneous universe) remains true. However, in Bianchi I

case this correction contains a *product* of Hubble parameters which can be positive when the *sum* of the Hubble parameters ( $h = 1/3(p + q + r)$ ) becomes zero and the condition  $h = 0$  no longer contradicts the constraint (6).

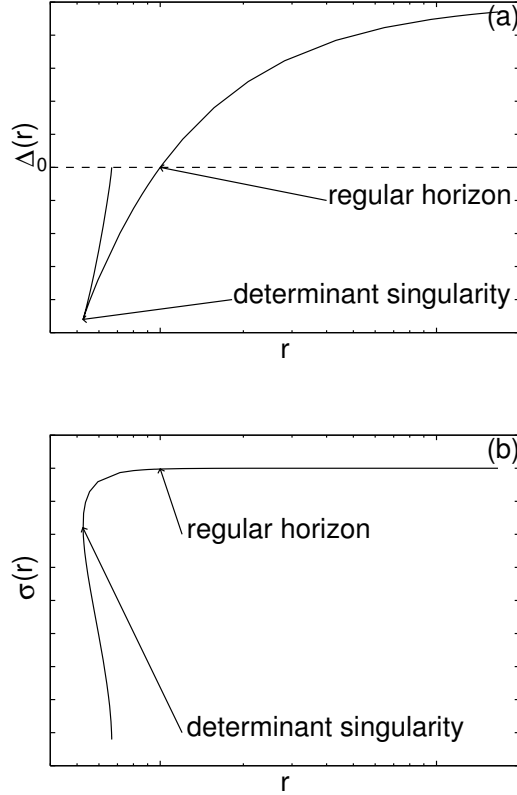


Figure 1. The behavior of the metric functions  $\Delta$  (presents as  $\partial^2\Delta/\partial r^2$  in field equations) and  $\sigma$  (presents as  $\partial\sigma/\partial r$  in field equations) against radial coordinate  $r$  in black hole case when the second order curvature corrections are taken into account

The equations of motion (6)–(10) can be integrated numerically. They have 5 degrees of freedom. Using constraint (6) one can reduce this number to 4. As it was done previously [5] we

calculate all dynamical variables checking the accuracy with the help of the constraint equation (6). In our calculation the left-hand side of the constraint equation did not exceed  $10^{-8}$  unless we are very close to an ordinary singularity. In all our numerical investigations we put  $\lambda = 1$  for simplicity.

The main determinant  $D_{main}$  is equal to:

$$\begin{aligned} D_{main} = & 3\lambda^4 e^{-8\phi} \dot{\phi}^2 r^2 p^2 q^2 \\ & - 2\lambda^3 e^{-6\phi} \dot{\phi} (p^2 q^2 r + p^2 q r^2 + p q^2 r^2) \\ & - 2\lambda^3 e^{-6\phi} \dot{\phi}^3 r p q \\ & - \lambda^2 e^{-4\phi} (p^2 q^2 + p^2 r^2 + q^2 r^2) \\ & + 2\lambda^2 e^{-4\phi} (p^2 r q + p q^2 r + p q r^2) \\ & + 2\lambda^2 e^{-4\phi} \dot{\phi}^2 (p q + p r + q r) \\ & - 2\lambda e^{-2\phi} \dot{\phi} (p + q + r) + 2 \end{aligned}$$

The determinant singularity occurs when  $D_{main}$  vanishes. Our numerical investigations show that it can happen for a rather wide set of initial data (see below). The asymptotic form of Hubble parameters behavior near this singularity  $t_s$  is (we checked it numerically and solved the equations on expansion coefficients  $h_{i\mu}$ , there are no any kinds of contradictions)

$$\begin{aligned} h_i &= h_{is} + h_{i1}\sqrt{t-t_s} + h_{i2}(\sqrt{t-t_s})^2 + \dots, \\ \phi &= \phi_s + \phi_1(\sqrt{r-r_s})^2 + \phi_2(\sqrt{r-r_s})^3 + (11) \end{aligned}$$

where  $h_i = p, q, r$  and  $t - t_s \ll 1$ .

Comparing (11) with (4) we can see that these two expansions are absolutely analogous. The expansion properties of functions having the same maximal derivative order in the equations of motion (the first order for  $\sigma$  and  $h_i$ , the second order for  $\Delta$ , and  $\phi$ ) are identical. It means that the properties of the determinant cosmological singularity are the same as the properties of the determinant Schwarzschild black hole singularity (keeping in mind, of course, that metric functions in cosmological case depend on time while in black hole they depend on the radial coordinate).

A numerical example is plotted in Fig. 2. Again, we can see two branches of solution and we can not continue these solutions further in time.

In our investigation we calculated two-dimensional slices in  $(\alpha, \beta)$ -plane of initial condition space with fixed values of  $h$  and  $\phi$ . The ini-

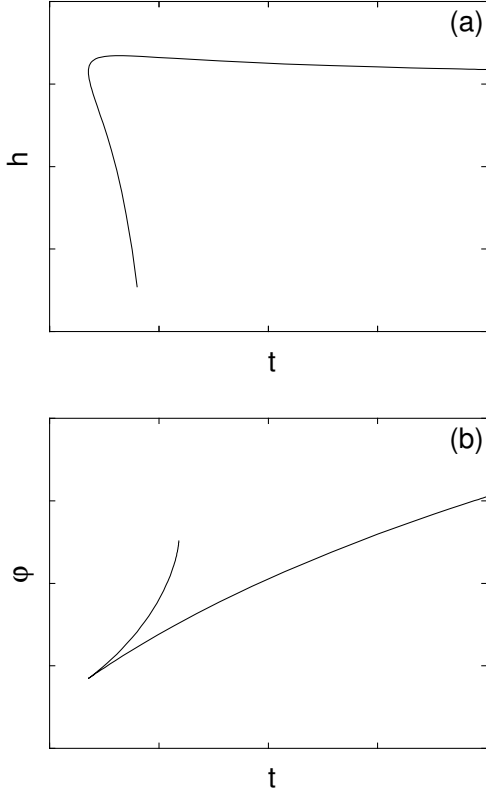


Figure 2. The behavior of the Hubble functions  $h_i$  (presents as  $\partial h_i / \partial t$  in field equations) and  $\phi$  (presents as  $\partial^2 \phi / \partial t^2$  in field equations) against coordinate  $t$  in Bianchi I case when the second order curvature corrections are taken into account

tial value of  $\dot{\phi}$  has been taken from the constraint equation, which is quadratic with respect to  $\dot{\phi}$ . The results below corresponds to the choice of the largest root of the quadratic equation. Each of the slices represent a  $100 \times 100$  grid. For each node of the grid we calculated both future and past solutions over the time interval of  $10^5$  in our units. There are three possible outcomes: ordinary singularity, determinant singularity and a nonsingular behavior. Such slices have been calculated for the values of  $\phi$  in the interval from  $\phi = -15$  to  $\phi = +15$  and for the values of  $h$  in

the interval from  $h = 1 \cdot 10^{-5}$  to  $h = 1$ .

Each of the numerical solutions has been analyzed and classified. Finally, for each slice we obtained picture like one shown in Fig. 4–6. Here the black color corresponds to non-singular solutions. The dark-gray color corresponds to ordinary singular solutions and the light-gray color corresponds to solutions with determinant singularity. The white color indicates prohibited regions in initial condition space where none of the solutions can start.

For large values of  $\phi$  the allowed region in  $(\alpha, \beta)$ -plane has a compact subregion of approximately circular shape with the center in point  $(0, 0)$  (see Fig. 4). This can be easily seen from constraint equation (6) if the term proportional to  $e^{-2\phi}$  is neglected. Numerical calculations show that in this case all future solutions are non-singular while all past solutions are singular with  $D_{main} \rightarrow 0$ . There is only one exception from this rule: the past solution for  $\alpha = \beta = 0$  (the isotropic case) has an ordinary singularity.

With decreasing of  $\phi$  this picture changes dramatically. The shape of allowed region undergoes substantial transformation (see Fig. 6): the former compact subregion becomes connected with the outer non-compact one. The more important feature is that some trajectories meet a singularity in future, either due to a recollapse (see above) or vanishing of the main determinant. The fraction of such solutions increases with initial  $\phi$  decreasing. For some value of initial  $\phi$  the solutions, nonsingular in future, disappear completely (apart from the exceptional isotropic case). This critical value depends on generalized Hubble parameter  $h$  as it is plotted in Fig. 3. The transition from the regime with only nonsingular future solutions to one with only singular future solutions is rather sharp according to our results which can be easily seen from Fig. 3. The universe with  $\phi < \phi_0$  (for a given  $h$ ) and an arbitrary small nonzero initial anisotropy can not leave a high-curvature regime and falls into a singularity, so such initial conditions are not suitable for describing the evolution of the our Universe.

The other important dynamical feature that was found via numerical integrations is related with past asymptotic. Though both described

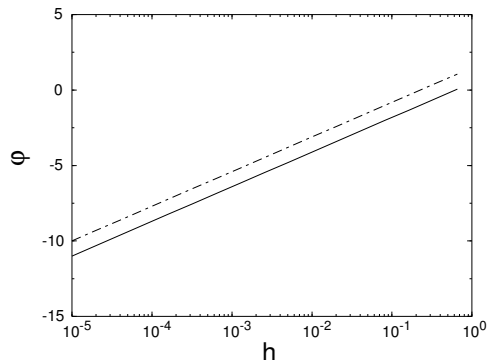


Figure 3. The minimal initial values of  $\phi$  which allow solutions non-singular in future (solid line) and the maximal initial values of  $\phi$  which allow singular solutions in future (dot-dashed line).

types of singularity are valid for various initial data sets, all the initial data which lead to non-singular future behavior have determinant singularity in the past (again, we ignore the exceptional isotropic solution). In particular, for large initial  $\phi$  the only possible past singularity is the determinant singularity (Fig. 4).

To obtain this result we investigated a rather wide set of initial conditions. However, the full set of allowed initial conditions is noncompact and, hence, we have no proof of this statement in the strict sense. Hence, we can put forward a **conjecture**: *the past singularity for nonsingular in future Bianchi I cosmological model with the second order curvature corrections is of determinant type*. This proposal is analogous to the result obtained in [5] for Schwarzschild black hole, where the asymptotically Minkowski initial data at infinity lead to a determinant singularity at the finite values of the radial coordinate.

### Acknowledgments

This work was supported via 'Universities of Russia, Fundamental Investigation' grant no 990777 and, partially supported by Russian Foundation for Basic Research via grants no 99-02-

16224 and 00-15-96699. Authors are grateful to H.-J.Schmidt for comments.

### REFERENCES

1. S.W. Hawking and G.F.R. Ellis, "Large Scale Structure of Space-Time", *Cambridge University Press, Cambridge*, (1973); S.W. Hawking and R. Penrose, *The Nature of Space and Time, Princeton, USA, University Press*, 141 p. (1996) (The Isaac Newton Institute series of lectures).
2. E.S.Fradkin and A.A.Tseytlin, *Phys. Lett. B* **158**, 316 (1985), *Nucl. Phys. B* **262**, 1 (1985); A.Sen, *Phys. Rev. D* **32**, 2102 (1985); D.J.Gross and J.H.Sloan, *Nucl. Phys. B* **291**, 41 (1987).
3. S. Mignemi and N.R. Stewart, *Phys. Rev. D* **47**, 5259 (1993); M. Natsuume, *Phys.Rev. D* **50**, 3945 (1994).
4. P. Kanti, N.E. Mavromatos, J. Rizos, K. Tamvakis and E. Winstanley, *Phys. Rev. D* **54**, 5049 (1996), **D 57**, 6255 (1998); T. Torii, H. Yajima and K. Maeda, *Phys. Rev.D* **55**, 739 (1997).
5. S.O. Alexeyev and M.V. Pomazanov, *Phys. Rev. D* **55**, 2110 (1997); S.O. Alexeyev and M.V. Sazhin, *Gen. Relativ. and Grav.* **30**, 1187 (1998).
6. D.L. Wiltshire, *Phys. Rev. D* **38**, 2445 (1988), *Phys. Lett. B* **169**, 36 (1985).
7. F.J.Tipler, *Phys. Lett. A* **64**, 8 (1977).
8. M.V.Pomazanov, 'On the Structure of Some Typical Singularities for Implicit Ordinary Differential Equations', Preprint math-ph/0007008.
9. L.M.Krauss and M.S.Turner, *Gen. Relativ. and Grav.* **31**, 1453 (1999).
10. W.Puszkarcz, *Phys. Lett. B* **226**, 39 (1989); M.Demianski, Z.Golda, W.Puszkarcz, *Gen. Relativ. and Grav.* **23**, 917 (1991).
11. T.Kitaura and J.T.Wheeler, *Phys. Rev. D* **48**, 667 (1993).
12. S. Kawai and J. Soda, *Phys. Rev. D* **59**, 063506 (1999). [gr-qc/9807060].
13. H. Yajima, K. Maeda and H. Ohkubo, *Phys. Rev. D* **62**, 024020 (2000). [gr-qc/9910061].

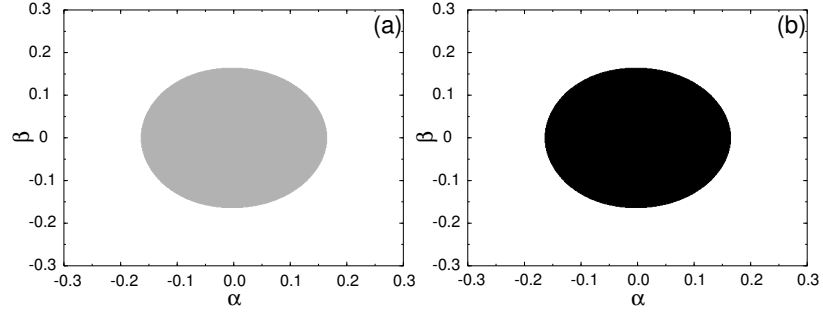


Figure 4. A slices of initial condition space in  $(\alpha, \beta)$ -plane for  $h = 0.16$  and  $\phi = 0$ . Figure (a) corresponds to the past solutions and figure (b) corresponds to the future solutions. The black color corresponds to non-singular solutions, the dark-gray color corresponds to ordinary singular solutions and the light-gray color corresponds to solutions with determinant singularity. The white color indicates prohibited regions in the initial condition space.

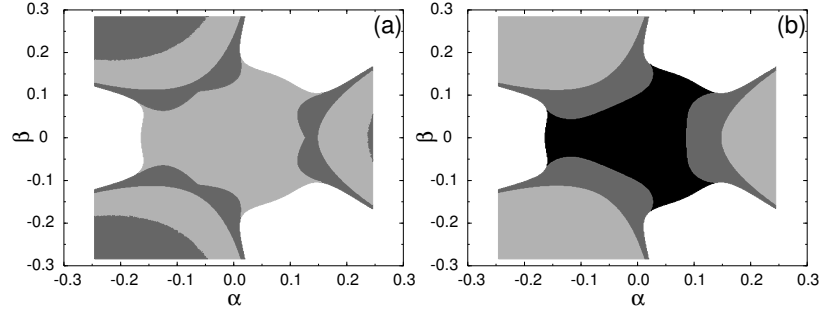


Figure 5. The similar slices for  $h = 0.16$  and  $\phi = -1$ .

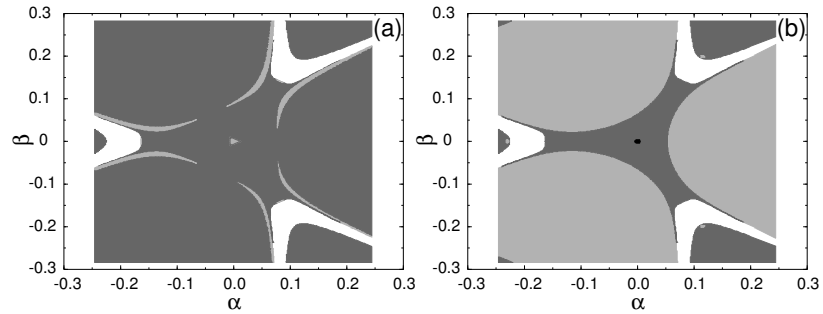


Figure 6. The similar slices for  $h = 0.16$  and  $\phi = -2$ .